ISSN 0016-7029, Geochemistry International, 2013, Vol. 51, No. 11, pp. 889-895. © Pleiades Publishing, Ltd., 2013.
Original Russian Text © V.A. Zaitsev, L.N. Kogarko, V.G. Senin, 2013, published in Geokhimiya, 2013, Vol. 51, No. 11, pp. 987-994.

Phase Equilibria in the System Lamprophyllite—Nepheline

V. A. Zaitsev, L. N. Kogarko, and V. G. Senin

Vernadsky Institute of Geochemistry and Analytical Chemistry, Russian Academy of Sciences, ul. Kosygina 19, Moscow, 119991 Russia

e-mail: alkaline@geokhi.ru

Received October 26, 2012; in final form, April 10, 2013

Abstract—Experimental studies of the melting diagram for the lamprophyllite—nepheline system and data on the phases crystallizing in this system indicate that lamprophyllite incongruently melts with the origin of melt and titanium oxide. The maximum temperature at which nepheline and lamprophyllite can occur in equilibrium is estimated at 833 ± 6°C.

Our pioneering data on lamprophyllite crystallization from melt prove that this mineral can be of magmatic genesis. The distribution coefficients between lamprophyllite and melt are evaluated for K (0.1—0.25), Mn (0.82-1.06), Fe (0.13-0.40), and Mg (0.82-1.5); and the Sr/Ba lamprophyllite/melt exchange coefficient is estimated at 1.8—3.7.

Keywords: titanosilicates, melting curves diagram, lamprophyllite, nepheline, titanosilicate melts, phase equilibria, distribution coefficients, tausonite, freudenbergite, rutile

DOI: 10.1134/S0016702913110104

INTRODUCTION

Alkaline rocks, first of all their agpaitic varieties, are typically rich in titanium and sometimes contain numerous and diverse titanium minerals, including more than 150 species of titanosilicates. Thanks to this diversity, titanosilicates can be utilized as sensitive indicators of the crystallization conditions. Interpretations of the information recorded in naturally occurring titanosilicates are based on experimental data on the crystallization fields of these minerals.

Information on the stability of titanosilicates at low temperatures is intensely accumulated thanks to numerous experiments on the hydrothermal synthesis of mesoporous titanosilicates. Analogues of minerals recently obtained by hydrothermal synthesis include ivanyukite-Na-Ti $Na_3[Ti_4(OH)_3(SiO_4)_3] \cdot 7H_2O$ [1], sitinakite $Na_2KTi_4Si_2O_{13}(OH) \cdot 4H_2O$ [2], and others. Identity between mesoporous ltsilsi and the following mineral phases was proved: ETS-4 and zorite $Na_6Ti_5Si_{12}O_{34}(O,OH)_5 \cdot 11H_2O$ [3], titanosilicate AM-2 $K_2TiSi_3O_9 \cdot H_2O$ and ubite [4], and AM-3 and penkvilksite $Na_4Ti_2Si_8O_{22} \cdot 4H_2O$ [5].

Much less information is currently available on higher temperature equilibrium between titanosilicates and melts. The melting diagram for the $Na_2O—TiO_2—SiO_2$ system studied in [6, 7] can describe melting only of the simplest phases, such as paranatisite $Na_2TiSi_2O_7$, lorenzenite $Na_2Ti_2Si_2O_9$, and narsarsukite Na_2TiSiO_5.

Our research was centered on the temperature stability limits of minerals of the lamprophyllite group $(Sr,Ba,K,Na)_2Na(Na,Fe,Mn)_2Ti[Ti_2(Si_2O_7)_2]O_2(OH,F,O)_2$, which are widespread phyllosilicates of agpaitic rocks. For this purpose, we have studied the melting of lamprophyllite and phase relations in the lamprophyllite—nepheline system, because minerals of the lamprophyllite group always occur in association with nepheline [8].

METHODS AND MATERIALS

The starting materials were a lamprophyllite sample in pegmatite from the Lovozero Massif, Kola Peninsula, and partly recrystallized synthetic glass whose composition corresponded to nepheline $NaAlSiO_4$. Their compositions are presented in Table 1. The material for the experiment was prepared by triturating together the lamprophyllite and glass.

The pulverized material was then welded in Pt ampoules, which were held in vertical electric furnaces with Ni—Cr and Pt heaters and then quenched in iced water. The experiments typically lasted from 5 to 360 h. The temperature was measured by a Pt—Rh thermocouple, which was calibrated against the melting points of NaCl and KCl. The temperature was measured accurate to ±15°C.

The experiments were conducted by approaching equilibrium either from above (the ampoule with the experimental charge was heated to 1000—1100°C and then cooled to the experimental temperature or quenched and then heated to the required temperature) or from below (the ampoules were not preliminarily heated).

The redox conditions of the experiments were not controlled because the low iron concentrations provide sound grounds to believe that the phase relations

Table 1. Composition of starting materials used in the experiments

Component	Lamprophyllite	Nepheline*
SiO_2	31.78	42.30
TiO_2	29.49	-
Al_2O_3	0.17	35.88
FeO	2.15	-
MnO	4.02	-
MgO	0.63	-
CaO	0.87	-
SrO	15.05	-
BaO	1.05	-
Na_2O	12.07	21.81
K_2O	0.49	-
Nb_2O_5	0.21	-
F	2.05	-
Total	100.03	100

Synthetic partly recrystallized glass of nepheline composition.

(except only for the iron—titanium oxides) should be independent of oxygen pressure.

The phase composition of the samples was determined in immersion liquids. The phases were analyzed on a Cameca SX-100 (France) X-ray spectral microprobe equipped with four crystal-diffraction spectrometers, at an accelerating voltage of 15 kV and a beam current of 30 nA. The samples were sputter coated with carbon in vacuum.

Difficulties encountered in the course of microprobe analysis for F and Na stem from the volatility of these elements under an electron beam. In order to minimize this effect, we applied a beam defocused to 5 um in diameter and an unvarying measuring procedure of the X-ray intensities of elemental peaks, with F and Na being the first to analyze [9, 10].

EXPERIMENTAL RESULTS

The experimental products contained glass, lamprophyllite $(Sr, Ba, K, Na)_2Na(Na, Fe, Mn)_2Ti[Ti_2(Si_2O_7)_2]O_2(OH, F, O)_2$, rutile TiO_2, tausonite $Sr_{1-x}Na_xTiO_{3-x}F_x$, freudenbergite $Na_2Fe^{1}_{1.2}Ti^{6}_{1.7}O_{16}$, nepheline $NaAlSiO_4$, magnetite Fe_3O_4 (in a single experiment), a complex titanate of the composition $(Ba, Na)_2Mn_4(Ti, Fe)_8O_{21}$, and an unidentified leucocratic phase. The phase relations are illustrated in Fig. 1.

The examined lamprophyllite—nepheline melting diagram is pseudobinary. Inasmuch as the composition of the oxides crystallizing in the lamprophyllite—nepheline system does not lie on the lamprophyllite—nepheline join, the composition of melt in equilibrium with them cannot be adequately described within the lamprophyllite—nepheline system.

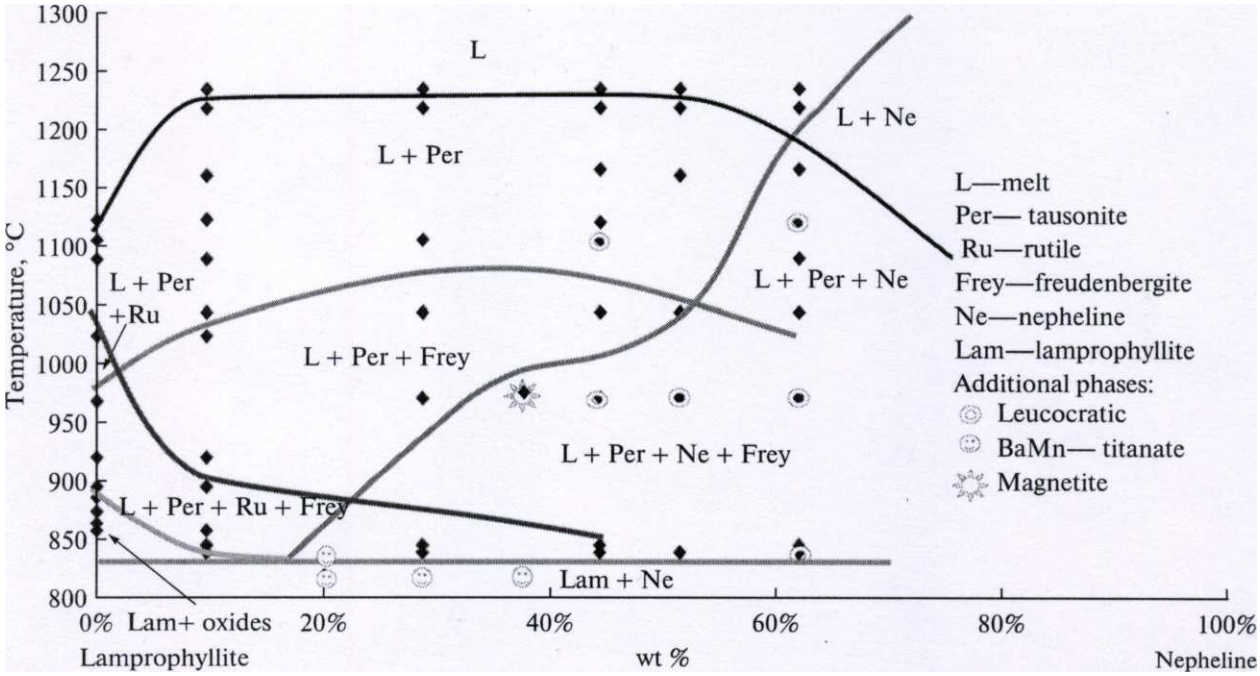

Fig. 1. Lamprophyllite—nepheline melting diagram.

Table 2. Composition (wt %) of F-bearing

Starting material	T, °C	Component, wt %														
		Na_2O	MgO	Al_2O_3	SiO_2	K_2O	CaO	TiO_2	MnO	FeO	SrO	Nb_2O_5	BaO	F	Total	$-O=F_2$
20% Ne 80% Lam	812	2.06	0.02	0.29	1.63	0.01	1.94	42.02	0.29	0.26	49.15	0.72	0.33	1.10	98.72	98.26
	812	2.10	0.02	0.36	1.28	0.01	1.93	43.22	0.30	0.13	49.94	0.76	0.31	1.43	100.36	99.76
	827	1.28	0.00	0.03	0.00	0.01	1.75	45.64	0.07	0.12	50.38	1.03	0.13	0.25	100.44	100.33
	827	1.43	0.02	0.08	0.11	0.00	1.78	45.30	0.04	0.21	48.88	1.02	0.18	0.08	99.05	99.02
28% Ne 72% Lam	812	1.45	0.02	0.08	0.21	0.02	1.74	42.94	0.19	0.26	50.12	1.08	0.31	1.06	98.42	97.97

Starting material	T, °C	Cations p.f.u.														
		Na	Mg	Al	Si	K	Ca	Ti	Mn	Fe	Sr	Nb	Ba	F	O*	O + F
20% Ne 80% Lam	812	0.12	0.00	0.01	0.05	0.00	0.06	0.91	0.01	0.01	0.82	0.01	0.00	0.10	2.88	2.98
	812	0.12	0.00	0.01	0.04	0.00	0.06	0.93	0.01	0.00	0.83	0.01	0.00	0.13	2.86	2.99
	827	0.07	0.00	0.00	0.00	0.00	0.05	1.00	0.00	0.00	0.85	0.01	0.00	0.02	2.97	3.00
	827	0.08	0.00	0.00	0.00	0.00	0.06	1.00	0.00	0.01	0.83	0.01	0.00	0.01	2.98	2.99
28% Ne 72% Lam	812	0.08	0.00	0.00	0.01	0.00	0.06	0.96	0.00	0.01	0.86	0.01	0.00	0.10	2.90	3.00

Tausonite, a Sr—Ti mineral of the perovskite group, is the first phase to crystallize in most of the compositions. It develops as cubic crystals or, more rarely, fluorite-law twins. The size of the crystals varies from experiment to experiment. Representative microprobe analyses of the tausinite are reported in Table 2. The recalculation of these analyses and their normalization to two metal atoms shows that the synthetic tausonite contains 0.77-0.87 f.u. Sr, 0.1-0.2 f.u. Na, 0.9-1.0 f.u. Ti, up to 0.05 f.u. Nb, up to 0.02 f.u. Fe, and up to 0.25 f.u. F.

Naturally occurring tausonite was described in ultragpaitic rocks from the Murun massif [11] as brown equant crystals up to 5 mm. Along with Si and Ti, it contains 0.8-0.16 f.u. Ca, 0.05-0.2 f.u. Na, up to 0.2 f.u. REE, and 0.01 f.u. Nb and is a series between the tausonite and perovskite end members: Me^{2+} + Ti —> Na + Nb (lueshite) and Sr + Ti -> $Na_{0.5}$ + TR0.5 + Ti (loparite).

Our synthetic tausonite contains virtually no REE (they were not introduced into the system) and Nb (0.05 f.u.) but contains up to 0.2 f.u. Na. It is worth mentioning that the synthetic tausonite contains up to 1.5 wt % F. The Na and F concentrations are positively correlated and are equal (if expressed in formula units). Thus, the formula of the synthetic tausonite can be written as $Sr_{1-x}Na_xTiO_{3-x}F_x$. This led us write the formula of the sodic end member as $NaTiO_2F$. The concentration of this end member in the synthesized crystals reaches 20 mol %.

The compound $NaTiO_2F$, which undergoes a phase transition at 950°C and decomposes at 1070°C, was discovered in the TiO_2—NaF system [13] but was not confirmed by the latest studies [14].

Natural minerals of the perovskite group are commonly not analyzed for F, and rare analyses listing this element show its concentrations no higher than 0.03 wt %. The only exception is a lueshite analysis containing 0.1 wt % F [15].

The presence of $NaTiO_2F$ as an isomorphic component in tausonite suggests that minerals of perovskite structure can play a certain part in F budget. In particular, it is reasonable to think that F can occur in the perovskite solid solution under lower mantle conditions.

The occurrence of F in perovskite should first of all hamper the accommodation of HFSE in the structure of the mineral, for example, Nb and Ta at octahedral sites and/or REE at cuboctahedral ones. Correspondingly, high F concentrations should suppress their distribution coefficients between perovskite and melt.

It is pertinent to mention a temperature maximum in the central part of the liquidus line of tausonite, in spite of the fact that the concentrations of components in it decrease from the lamprophyllite to nepheline composition. An increase in the crystallization temperature of tausonite with a decrease in the Ti concentration in the melt can be explained by and increase in the activity coefficient due to the strong polymerization of the melt. This can be illustrated by a change in the

Table 3. Composition (wt %) of natural and synthetic freudenbergite

Component	Katzenbuckel		Khibina	Dal'nyaya pipe	Synthesized in experiments*						
	Low-Ti	High-Ti			100% Lam 915°C	37% Ne 63% Lam 971°C			10% Ne 90% Lam 851°C		
SiO_2	0-0.01	0	—	—	0.81	0.17	0.62	0.52	0.66	0.06	0.89
TiO_2	64.59-71.35	69.72-76.06	78.05-81.46	77.4-80.4	78.56	76.38	76.01	76.21	79.26	79.60	75.22
ZrO_2	0.01-0.69	0-0.51	0-0.45	0-0.06		-	-	-	-	-	-
Nb_2O_5	0.5-5.97	0.77-12.32	0-0.26	0.04-1.11	0.00	0.05	0.00	0.06	0.05	0.00	0.09
V_2O_5	—	-	0-0.51	-	-	-	-	-	-	-	-
Al_2O_3	0	0	0.14-0.14	0.71-1.09	0.00	0.43	0.49	0.47	0.04	0.05	0.17
Cr_2O_3	0-0.05	0-0.03	0-0.37	0.47-1.92	-		-	-	-	-	-
Fe_2O_3*	15.69-20.56	6.35-11.32	10.04-12.73	5.53-8.99	7.64	7.85	7.83	7.88	10.69	10.67	10.53
MnO	0.05-0.63	0.63-1.42	0.04-0.12	0	3.53	2.84	2.79	2.69	2.29	2.50	2.56
ZnO	0.03-0.19	0.36-0.89	-	-	-	-		-	-	-	-
MgO	0.44-1.36	1.54-2.49	0.39-0.96	1.45-3.16	0.92	1.23	1.19	1.20	0.73	0.75	1.00
CaO	0-0.07	0.01-0.05	0.04-0.06	0.13-0.93	0.00	0.11	0.11	0.12	0.08	0.06	0.00
Na_2O	8.1-8.93	6.7-8.82	8.15-9.75	8.05-8.67	7.24	7.71	7.74	7.61	7.26	7.62	8.74
K_2O	0-0.07	0.01-0.02	0-0.04	0-0.15	0.05	0.01	0.01	0.02	0.03	0.02	0.06
BaO	—	—	—	-	0.00	0.12	0.00	0.08	0.14	0.00	1.18
SrO	-	-	-	-	0.56	0.92	0.62	0.72	0.25	0.15	0.28

* Normalized to 10 cations, the phase contains 6.5—7.4 f.u. of Ti, 1.7-2 f.u. of Na; 0.4-0.9 f.u. of Fe, 0.25-0.4 f.u. of Mn, and 0.2 f.u. of Mg.

NBO/T ratio, which is zero for the nepheline composition[1] and four for the lamprophyllite one.

Rutile occurs as needles, which seem to be alternatively pinkish and greenish or bluish in immersion liquids because of their small sizes and high birefringence and show straight extinction. Microprobe analyses indicate that the rutile contains up to 4 wt % Nb_2O_5.

The crystallization temperature of rutile is at a maximum in left-hand portion of the system and rapidly decreases with the amount of nepheline added to the system. The liquidus line of freudenbergite behaves in the opposite way: the crystallization temperature of this mineral has a maximum in the central part of the diagram.

An increase in the crystallization temperature of freudenbergite with an increase in the content of the nepheline component in the system in the left-hand part of the diagram cannot be explained by a decrease in the titanium solubility with increasing degree of melt polymerization, because the crystallization temperature of rutile decreases within this range. The relations can rather be interpreted as resulting from the reaction rutile + melt = freudenbergite, which is shifted to its right-hand side with increasing Na concentration in the melt.

FVeudenbergite forms prismatic crystals, which are reddish brown in immersion liquids and show straight extinction and high birefringence, with these features corresponding to the optics of freudenbergite from the Katzenbuckel Complex [17].

Naturally occurring freudenbergite is a solid solution of two end members $Na_2Fe^{2+}Ti_6O_{16}$ and $Na_2Fe^{2+}Ti_7O_{16}$, which were referred to as low- and high-Ti freudenbergite, respectively [16]. The mineral was also described as ***freudenbergite sensu stricto*** and ***ferrous analog of freudenbergite*** in [18]. Both varieties were found in the course of close examination of samples from the Katzenbuckel Complex, Germany, in which this mineral was documented for the first time [19].

As a secondary metasomatic mineral high-Ti freudenbergite was found in lower crustal granulites in Liberia and in an upper mantle xenolith from South Africa. It was also found as inclusions in ilmenite megacrysts from the Dal'nyaya pipe, Yakutia, and low-Ti freudenbergite was identified as surrounding rutile xenocrysts in a kimberUte dike in the Urukit field in Yakutia [18] and in a large metasomatized xenolith in the Khibina Massif [19].

Representative analyses of freudenbergite synthesized in the lamprophyllite—nepheline system are comparable, with regard for compositional variations, with

[1] Following [4], we calculated NBO/T as (2O — 4T)/T, where O is the total number of O atoms calculated from the stoichiometry of the metals, and T is the number of tetrahedrons, which is equal to the total number of Si + Al + Fe).

Table **4.** Composition (wt %) of newly formed lamprophyllite and glass in equilibrium with it

Component	Lamprophyllite				Glass			
	Starting material							
	100% Lam	20%Ne 80%Lam	28%Ne 72%Lam	28%Ne 72%Lam	1 ппо/т IUUTbLam	20%Ne 80%Lam	28%Ne 72%Lam	28%Ne 72%Lam
	851°C	812°C	812°C	798°C	851°C	812°C	812°C	798°C
SiO_2	31.78	28.45	30.125	28.955	49.89	47.54	51.97	58.15
TiO_2	29.49	31.5	30.31	28.79	19.26	11.62	7.46	7.41
Al_2O_3	0.17	0.29	0.22	0.275	0.51	9.79	11.24	11.44
FeO	2.15	0.68	0.46	0.59	6.76	2.32	3.51	1.99
MnO	4.02	4.28	4.93	4.955	4.36	5.26	4.67	4.76
MgO	0.63	0.66	0.785	1.02	0.67	0.85	0.54	0.80
CaO	0.87	0.79	0.8	0.565	n.a.	1.19	1.06	0.54
SrO	15.05	16.47	18.06	18.05	4.72	2.21	1.95	2.12
BaO	1.05	1.53	1.41	2.175	0.56	0.53	0.28	0.95
Na_2O	12.07	10.98	11.16	10.835	4.05	11.86	11.43	9.62
K_2O	0.49	0.04	0.075	0.055	1.28	0.14	0.68	0.63
Nb_2O_5	0.21	0.07	0.095	0.065	2.56	0.16	0.26	0.04
F	2.05	2.29	3.13	3.085	n.a.	5.30	3.70	1.70
Total	100.03	98.01	101.56	99.42	94.60	98.77	98.73	100.15
Sr/Ba	23.0	14.9	19.0	12.3	12.5	6.2	10.4	3.3

analyses of natural freudenbergite in Table 3. The Ti concentration in our synthetic freudenbergite is as in high-Ti freudenbergite varieties, but our mineral is notably richer in Mn.

The Ti concentration of freudenbergite increases with increasing temperature, whereas the Fe and Mn concentrations simultaneously decrease.

Newly formed **lamprophyllite** was identified in the products of our experiments approaching equilibrium from above at temperatures no lower than 881°C. The mineral occurs as large (up to 1 mm) prismatic crystals of pale yellow to greenish color, containing inclusions of titanates. Newly formed lamprophyllite was also found in some products of our experiments approaching equilibrium from below.

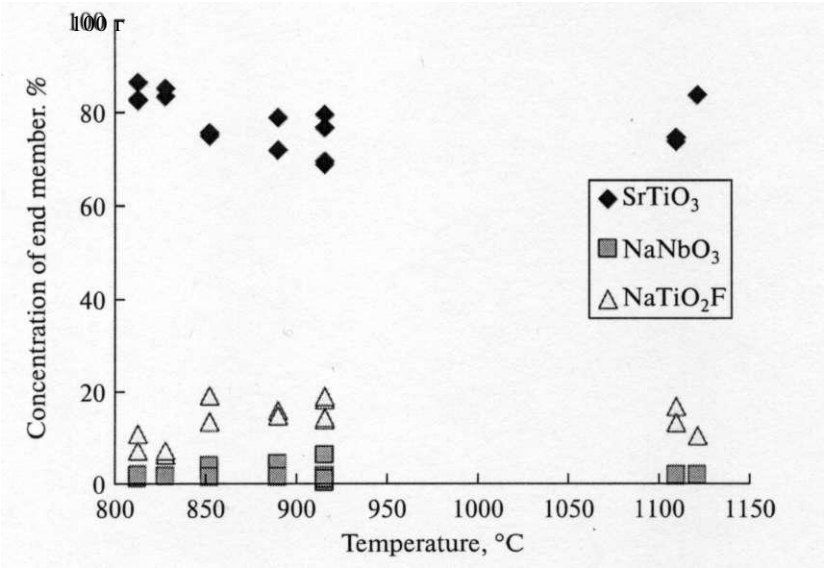

Fig. **2.** Dependence of tausonite composition on temperature (the concentration of the fluorine end member is calculated from the Na concentration).

Table 4 presents analyses of the newly formed lamprophyllite. The newly formed lamprophyllite clearly differs from the primary lamprophyllite, whose relics were identified in the experiments "from below" in containing less K and Fe but more Mn.

The lamprophyllite—melt equilibrium temperature likely lies between 881°C (at which it crystallizes in experiments) and 915°C (at which no relics can be preserved).

Nepheline was found as equant crystals with low birefringence. It contains excess silica, because its formula (normalized to four O ions) can be written as $(Na^{0.91-0.95}K0.01-0.04)Al0.94-0.97Fe0.00-0.01\ Si1.02-1.06O4$ The concentration of excess Si is much lower than could be expected for this temperature range from the $NaAlSi0^4$-$KAlSi0^4$-$Si0^2$ diagram [20]. This can be explained by the fact that the nepheline thermometer was calibrated under the assumption that nepheline occurs in equilibrium with albite, whereas the silica activity in our experiments was much lower.

The **glass** examined in our experimental products is pale brown, with a high (>1.640) refraction index. The composition of the glass remarkably varies depending on temperature and the composition of the starting material.

Table 4 reports the composition of the glass obtained in our experiments "from above", in which we have analyzed the newly formed lamprophyllite. Unfortunately, the distribution of crystals in the glass does not always allow analysis with a defocused beam. As is known, this is particularly important when alkali-rich glasses are analyzed, whose structure is favorable for the active migration of ions during analysis, and this leads to the loss of alkalis and distortion of the actual composition and analytical totals.

These data can nevertheless be utilized to evaluate the distribution coefficients between lamprophyllite and melt for certain minor components. These coefficients are 0.1-0.25 for K, 0.82-1.06 for Mn, 0.13-0.40 for Fe, and 0.82—1.5 for Mg. These values are close to estimates from the composition of lamprophyllite microlites and glass in combeite nephelinite [21]: 0.29 for K, 0.74 for Mn, 0.18 for Fe, and 1.06 for Mg.

The Sr/Ba ratio of the lamprophyllite is 1.8—3.7 times higher than in the melt in equilibrium with it. This is consistent with the fact that lamprophyllite gives way to barytolamprophyllite with the transition from earlier to later rocks in alkaline massifs [8]. It follows that lamprophyllite crystallization from melt should result in its enrichment in Ba relative to Sr.

The association of lamprophyllite and nepheline was synthesized in our experiments approaching equilibrium from above at a temperature of 827°C. The products of these experiments at temperatures of 839°C and higher (depending on the bulk composition of the system) contain either lamprophyllite or nepheline. This led us to evaluate the temperature of their simultaneous crystallization at 833 ± 6°C. The temperature maximum in the system corresponds to approximately 20 wt % of the nepheline component.

Along with lamprophyllite and nepheline, the products of these experiments at temperatures below 833°C contain glass, tausonite, freudenbergite, and/or titanate whose formula can be written as $(Ba,Na)^2Mn^4(Ti,Fe)^80^21$. Hence, the incongruent melting of lamprophyllite is associated with the accommodation of much Ti and Sr in oxides and the enrichment of the melt in Na and Si. The compositions of all liquidus phases and melt plot outside the lamprophyllite—nepheline join. As the temperature decreases, crystallizing lamprophyllite overgrows some of the oxide minerals, first of all, tausonite. As a results, these minerals cease to react with the melt, which is in excess. The evolution of the melt during lamprophyllite and nepheline crystallization results in further enrichment in excess components.

CONCLUSIONS

The examined lamprophyllite—nepheline melting diagram is pseudobinary. Lamprophyllite melts incongruently, with the origin of melt and Ti oxides: rutile, tausonite, and freudenbergite. The titanates gradually give way to titanosilicates with decreasing experimental temperature, analogously to what takes place in natural alkali-rich systems.

Our experiments were pioneering in crystallizing lamprophyllite from melt and prove that this mineral can be of magmatic genesis. At the same time, the temperature of the simultaneous crystallization of lamprophyllite and nepheline in the examined system (833°C) should be regarded as the theoretical upper limit for the stability of the lamprophyllite—nepheline association. It is known that the addition of any new component to a system decreases the melting temperature of the system, and natural rocks always contain, along with nepheline and lamprophyllite, other minerals (feldspar, pyroxene, eudialyte, etc), and hence, the temperature at which lamprophyllite can crystallize in nature should be much lower than 833°C. Experimental data on phase relations in the course of melting of rocks of the Lovozero Massif suggest a solidus temperature close to 600°C [22].

Using the compositions of synthetic lamprophyllite and melt in equilibrium with it, we evaluated the distribution coefficients of trace elements and the exchange coefficients of Sr and Ba. The values thus obtained are close to the values obtained for combeite nephelinite from Oldonyo Lengai and correspond to the ubiquitous lamprophyllite replacement by Ba-rich members of the group in nature.

The phases synthesized in our experiments are close in composition to corresponding naturally occurring minerals. The most important difference between them is the higher F concentration of the tausonite, which

suggests that F can be accommodated in perovskite-group minerals in nature.

In spite of the unusual (and even exotic) composition of melts in the lamprophyllite—nepheline system, their uncommonly high NBO/T ratios and the high concentrations of alkalis and Ti in the crystallizing phases, the composition of the phases crystallizing in this system are close to the composition of the respective natural minerals. The distribution coefficients of elements for the lamprophyllite are also close to those occurring in nature, as also are the crystallization sequence of phases from melt. This proves that even such relatively simple synthetic systems can be adequately accurate in modeling the crystallization of titanosilicates in alkaline magmas.

ACKNOWLEDGMENTS

This study was financially supported by the Russian Foundation for Basic Research, project nos. 12-05-31254 and 11-05-12004-ofi-m, and Project NSH-2150.2012.5.

REFERENCES

1. A. I. Nikolaev, G. Yu. Ivanyuk, S. V. Krivovichev, V. N. Yakovenchuk, Ya. A. Pakhomovskii, L. G. Gerasimova, M. V. Maslova, E. A. Selivanova, D. V. Spiridonova, and N. G. Konopleva, "Nanoporous titanosilicates: crystal chemistry, setting in alkaline massifs, and outlooks for synthesis," \estn. Kol'sk Nauchn. Ts. Ross. Akad. Nauk, No. 3, 51-62 (2010).

2. D. G. Medvedev, T Akhilesh, C. Abraham, and J. Hanson, "Crystallization of sodium titanium silicate with sitinakite topology: evolution from the sodium nonatitanatc phase," Chcm. Mater. **16,** 3659-3666 (2004).

3. G. Cruciani, P. De. Luca, A. Nastro, and P. Pattison, "Rietveld refinement of the zorite structure of ETS-4 molecular sieves," Micropor. Mesopor. Mater. **21** (1—3), 143-153 (1998).

4. N. Dobelin and T Armbruster, "Microporous titanosilicate AM-2: Rb-exchange and thermal behaviour," Mater. Res. Bull. **42,** 113-125 (2007).

5. Liu Yunling, Du Hongbin, Zhou Fengqi, and PangWenqin, "Synthesis of a new titanosilicate: an analogue of the mineral penkvilksite," Chem. Commun., 1467—1468 (1997).

6. E. H. Hamilton and G. W. Cleek, "Properties of sodium titanium silicate glasses," J. Res. Nat. Bur. Stand. **61** (2), 89-47(1958).

7. F. P. Glasser and J. Marr, "Phase relations in the system Na_2O-T10,-SiO_2," J. Am. Ceram. Soc. **62** (1-2)', 42-47(1979).

8. V. A. Zaitsev and L. N. Kogarko, "Compositions of minerals of the lamprophyllite group from alkaline massifs worldwide," Gcochcm. Int. **40** (4), 355-364 (2002).

9. H. Sigurdsson, "Quantitative methods for microprobe analysis of sodium in natural and synthetic glasses," Am. Mineral. **66,** 547-552(1981).

10. V. V. Vilisov and N. P. Ifin, "Specifics of X-ray microanalysis of minerals for fluorine," Zh. Anal. Khim. **35**(8), 1530-1539(1980).

11. E. I. \brob'ev, A. A. Konev, Yu. V. Malyshonok, G. G. Afonina, and A. N. Sapozhnikov, "Tausonite $SrTiO_3$—a new perovskite-group mineral," Zap. \fceross. Mineral. O-va **113**(1), 86-89 (1984).

12. A. A. Konev, E. I. \brob'ev, and K. A. Lazebnik, ***Mineralogy of the Murun Alkaline Massif*** (Izd-vo NITs OIGGM, Novosibirsk, 1996) [in Russian].

13. V. N. Pavlikov, V. A. Yurchenko, E. S. Lugovskaya, L. M. Lopato, and S. G. Tresvyatskii, "NaF-TiO_2 System," Zh. Anal. Khim. **20** (11), 3076-3079 (1975).

14. V. B. Nalbandyan, "Interaction of titanium dioxide with sodium fluoride and carbonate," Russ. **J.** Inorg. Chem. **45** (4), pp. 510-514 [in Russian].

15. A. A. Kukharenko, M. P. Orlova, A. G. Bulakh, E. A. Bagdasarov, O. M. Rimskaya-Korsakova, E. I. Nefedov, G. A. Il'inskii, A. S. Sergeev, and N. B. Abakumova, ***Caledonian Complex of Ulirabasic Alkaline Rocks and Carbonatites of the Kola Peninsula and Northern Karelia (Geology, Mineralogy, and Geochemistry)*** (Nedra, Moscow, 1965) [in Russian].

16. B. O. Mysen, D. Virgo, and F. A. Seifert, "Redox equilibria of iron in alkaline earth silicate melts: relationships between melt structure, oxygen fugacity, temperature and properties of iron-bearing silicate liquids," Am. Mineral. **69,** 834-847(1984).

17. V. Stahle, M. Koch, C. A. McCammon, U. Mann, and G. Markl, "Occurrence of low-Ti and high-Ti freudenbergite in alkali syenite dikes from the Katzenbuckel \blcano, southwestern Germany," Can. Mineral. **40,** 1609—1627(2002).

18. **L** A. Taylor and N. Pokhilenko, "Ferrous freudenbergite in ilmenite megacrysts: a unique paragenesis from the Dalnaya Kimberlite, Yakutia," Am. Mineral. **82,** 991-1000(1997).

19. O. S. Yakovleva, "Mineral diversity of fenitized xenoliths in the Khibina Massif, Kola Peninsula," in ***Mineral Diversity: Study and Conservation*** (Zemyata and Khorata, Sofia, 2009), pp. 193-199 [in Russian].

20. D. L. Hamilton, "Nephelines as crystallization temperature indicators," J. Geol. **69,** 321-329 (1961).

21. J. B. Dawson and P. G. Hill, "Mineral chemistry of peralkaline combeite—lamprophyllite nephelinite from Oldonio Lengai, Tanzania," Mineral. Mag. **62** (2), 179—196(1998).

22. Kogarko, L.N., ***Genetic Problems of Agpaitic Magmas*** (Nauka, Moscow, 1977).

Translated by E. Kurdyukov